THE ASTROPHYSICAL JOURNAL, 474:414–425, 1997 January 1

TORQUE REVERSAL AND SPIN-DOWN OF THE ACCRETION-POWERED PULSAR 4U 1626−67

DEEPTO CHAKRABARTY,[1] LARS BILDSTEN,[2] JOHN M. GRUNSFELD,[3] DANNY T. KOH, THOMAS A. PRINCE, AND BRIAN A. VAUGHAN
Space Radiation Laboratory 220-47, California Institute of Technology, Pasadena, CA 91125;
deepto@space.mit.edu, bildsten@fire.berkeley.edu, jgrunsfe@ca1.jsc.nasa.gov, koh@srl.caltech.edu,
prince@srl.caltech.edu, brian@srl.caltech.edu

AND

MARK H. FINGER,[4] D. MATTHEW SCOTT,[5] AND ROBERT B. WILSON
Space Science Laboratory ES-84, NASA/Marshall Space Flight Center, Huntsville, AL 35812; finger@gibson.msfc.nasa.gov,
scott@gibson.msfc.nasa.gov, wilson@gibson.msfc.nasa.gov
Received 1996 March 25; accepted 1996 July 24

ABSTRACT

Over 5 yr of hard X-ray (20–60 keV) monitoring of the 7.66 s accretion-powered pulsar 4U 1626−67 with the *Compton Gamma Ray Observatory*/BATSE large-area detectors has revealed that the neutron star is now steadily spinning down, in marked contrast to the steady spin-up observed during 1977–1989. This is the second accreting pulsar (the other is GX 1+4) that has shown extended, steady intervals of both spin-up and spin-down. Remarkably, the magnitudes of the spin-up and spin-down torques differ by only 15%, with the neutron star spin changing on a timescale $|\nu/\dot{\nu}| \approx 5000$ yr in both states. The current spin-down rate is itself decreasing on a timescale $|\dot{\nu}/\ddot{\nu}| \approx 26$ yr. The long-term timing history shows small-amplitude variations on a 4000 day timescale, which are probably due to variations in the mass transfer rate. The pulsed 20–60 keV emission from 4U 1626−67 is well-fitted by a power-law spectrum with photon index $\gamma = 4.9$ and a typical pulsed intensity of 1.5×10^{-10} ergs cm^{-2} s^{-1}. The low count rates with BATSE prohibited us from constraining the reported 42 minute binary orbit, but we can rule out long-period orbits in the range 2 days $\lesssim P_{\rm orb} \lesssim$ 900 days.

We compare the long-term torque behavior of 4U 1626−67 to other disk-fed accreting pulsars and discuss the implications of our results for the various theories of magnetic accretion torques. The abrupt change in the sign of the torque is difficult to reconcile with the extremely smooth spin-down now observed. The strength of the torque noise in 4U 1626−67, $\sim 10^{-22}$ Hz^2 s^{-2} Hz^{-1}, is the smallest ever measured for an accreting X-ray pulsar, and it is comparable to the timing noise seen in young radio pulsars. We close by pointing out that the core temperature and external torque (the two parameters potentially relevant to internal sources of timing noise) of an accreting neutron star are also comparable to those of young radio pulsars.

Subject headings: accretion, accretion disks — binaries: close — pulsars: individual (4U 1626–67) — stars: neutron — X-rays: stars

1. INTRODUCTION

Early studies of X-ray pulsars accreting from disks found that the observed long-term spin-up timescale ($\tau_{\rm su} = |\nu_{\rm spin}/\dot{\nu}_{\rm spin}| \lesssim 10^4$ yr) was much less than the X-ray–emitting lifetime ($\tau_{\rm X} \gtrsim 10^6$ yr), implying that long-term spin-up cannot be the steady state behavior of these systems (Elsner, Ghosh, & Lamb 1980). The discovery of prolonged spin-down (Makishima et al. 1988) and subsequent additional torque reversals (Chakrabarty et al. 1994, 1995b) in GX 1+4 was a dramatic illustration of this for the source with the shortest spin-up time ($\tau_{\rm su} \approx 40$ yr). At the same time, it raised questions about what sets the timescale of the order of years for these torque sign reversals. In this paper, we report on observations of a torque reversal and extended spin-down in a second pulsar, 4U 1626−67.

The X-ray source 4U 1626−67 ($l = 321°$, $b = -13°$) was discovered in the 2–20 keV band by *Uhuru* (Giacconi et al. 1972). Subsequent 1.5–30 keV observations with *SAS 3* revealed 7.68 s pulsations (Rappaport et al. 1977) and provided a sufficiently accurate position (Bradt et al. 1977) from which to identify the optical counterpart, KZ TrA (McClintock et al. 1977). Optical pulsations with 2% amplitude were detected at the same frequency as the X-ray pulsations (Ilovaisky, Motch, & Chevalier 1978) and are understood as reprocessing of the pulsed X-ray flux by the accretion disk (Chester 1979). The system shows strong, correlated X-ray/optical flares every ≈1000 s that are of undetermined origin (Joss, Avni, & Rappaport 1978; McClintock et al. 1980; Li et al. 1980) and have no X-ray spectral changes (Kii et al. 1986). A ≈40 mHz quasi-periodic oscillation was detected in X-ray observations by *Ginga* and the *Advanced Satellite for Cosmology and Astrophysics* (*ASCA*) (Shinoda et al. 1990; Angelini et al. 1995), and has been recently detected in optical observations as well (Chakrabarty 1996a).

Further timing of the optical pulsations detected weak, persistent pulsations in a sidelobe of the "direct" (X-ray) pulse frequency, which were attributed to a beat frequency with a 42 minute binary orbit arising from reprocessing on

[1] Current address: Center for Space Research 37-561, Massachusetts Institute of Technology, Cambridge, MA 02139.
[2] Current address: Department of Physics and Department of Astronomy, University of California, Berkeley, CA 94720.
[3] Current address: NASA/Johnson Space Center, Code CB, Houston, TX 77058.
[4] *Compton Observatory* Science Support Center, NASA/Goddard Space Flight Center/Universities Space Research Association.
[5] Universities Space Research Association.

the companion surface (Middleditch et al. 1981). X-ray timing measurements have thus far failed to detect orbital Doppler shifts of the pulsar signal, placing an upper limit of $a_X \sin i < 8$ lt-ms on the size of a 42 minute orbit and of $f_X(M) < 10^{-6}\, M_\odot$ on the mass function (Shinoda et al. 1990). The optical limits on the companion's luminosity rule out the possibility of accretion from a conventional stellar wind (Chakrabarty 1996a). The most likely Roche lobe–filling companion consistent with the timing limits is a low-mass (0.02–0.06 $M_\odot$) degenerate He or CO dwarf; more massive stars require very unlikely inclination angles (see Verbunt, Wijers, & Burm 1990 for a complete discussion). Such a companion would make 4U 1626−67 similar to the few known ultracompact binaries ($P_{orb} \lesssim 80$ minutes; see Nelson, Rappaport, & Joss 1986), all of which consist of a collapsed primary and a hydrogen-depleted low-mass secondary. Those with neutron star primaries are the X-ray burst sources 4U 1820−30 and 4U 1916−05 (see Nelson et al. 1986), while those with white dwarf primaries are the six AM CVn binaries (see Warner 1995a, 1995b). Recent *ASCA* observations of 4U 1626–67 detected a strong complex of neon emission lines near 1 keV (Angelini et al. 1995) and may provide a further clue to the composition of the mass donor.

For more than a decade after its discovery, accretion was steadily spinning up 4U 1626−67 on a timescale $\tau_{su} \approx 5000$ yr. However, long-term 20–60 keV monitoring of the source with the Burst and Transient Source Experiment (BATSE) on board the *Compton Gamma Ray Observatory* beginning in 1991 April found that the accretion torque had changed sign, causing spin-down at nearly the same rate (Wilson et al. 1993; Bildsten et al. 1994). This change of state was subsequently confirmed in 3–60 keV observations with the ART-P instrument on board *Granat* (Lutovinov et al. 1994), 0.2–2.4 keV observations with *ROSAT*/PSPC (Angelini, Ghosh, & White 1994), and 0.5–10 keV observations with *ASCA* (Angelini et al. 1995). In this paper, we report on over 5 yr of continuous BATSE timing and spectral data.

2. OBSERVATIONS AND ANALYSIS

2.1. *Pulse Frequencies*

BATSE is a nearly continuous all-sky monitor of 20 keV–1.8 MeV hard X-ray/γ-ray flux (see Fishman et al. 1989 for a description). Our standard BATSE pulsed source detection and timing analysis uses the 20–60 keV channel of the 4 channel/1.024 s resolution DISCLA data type (see Chakrabarty et al. 1993; Chakrabarty 1996b), and we reduce all of our timing observations to the solar system barycenter using the Jet Propulsion Laboratory DE-200 solar system ephemeris (Standish et al. 1992). The barycentric pulse frequency history of 4U 1626−67 from 1991 April to 1996 June was determined by dividing the BATSE data into short (a few days) segments and searching the Fourier power spectrum of each segment for the strongest signal in a small range around a pulse period of 7.7 s. The length of data used was always much shorter than the timescale for signal decoherence caused by the large pulse frequency derivative ($\tau_{decoh} = (1/|\dot{\nu}|)^{1/2} \approx 13$ days; see Appendix).

Figure 1 shows the pulse frequency history of 4U 1626−67. The pre-BATSE pulse-timing measurements are summarized in Table 1. (Optical pulse-timing observations are omitted because of their comparatively large measurement uncertainties.) During 1977–1989, the source underwent steady spin-up at a mean rate $\dot{\nu} = 8.54(7) \times 10^{-13}$ Hz s^{-1}. The pulse frequency history observed by BATSE from 1991 April to 1996 June (MJD 48360–50260) is also shown in Figure 1. The BATSE measurements are of comparable or better quality to the previous observations but have substantially better coverage in time. Throughout the BATSE observations, the pulsar was spinning down steadily at nearly the same rate that it had been previously spinning up. The data in the interval MJD 48600–48800 are of reduced quality as the result of telemetry problems and gaps associated with the failure of the tape recorder on board *Compton*. The overall BATSE history shows a significant quadratic component and is well-fitted (reduced $\chi^2 = 1.56$ with 366 dof) by

$$\nu(t) = \nu_0 + \dot{\nu}_0(t - t_0) + \tfrac{1}{2}\ddot{\nu}(t - t_0)^2 , \quad (1)$$

with $\nu_0 = 0.13048866479(1669)$ Hz, $\dot{\nu}_0 = -7.175647(4124) \times 10^{-13}$ Hz s^{-1}, and $\ddot{\nu} = 8.8020(1194) \times 10^{-22}$ Hz s^{-2}, referenced to the epoch $t_0 =$ MJD 49000 TDB. Extrapolating

TABLE 1

PRE-BATSE TIMING OBSERVATIONS OF 4U 1626−67

EPOCH		PULSE PERIOD		
Date	MJD	(s)	INSTRUMENT	REFERENCE
1977 Mar 24.4	43226.4	7.6806273(5)	*SAS3*	1
1978 Mar 29.7	43596.7	7.679190(25)	*HEAO 1*	2
1978 May 30.1.....	43658.1	7.67893(2)	*SAS 3*	3
1979 Feb 24.6	43928.6	7.677765(64)	*Einstein*	4
1979 Mar 10.1	43942.1	7.677565(24)	*Einstein*	4
1979 Mar 14.0	43946.0	7.677632(13)	*Einstein*	4
1982 Jul 4.0	45154.0	7.67271(3)	*Hakucho*	5
1983 May 4.0	45458.0	7.671350(1)	*Tenma*	6
1983 Aug 30.9	45576.9	7.67077(1)	*EXOSAT*	7
1986 Mar 31.0	46520.0	7.6664220(5)	*EXOSAT*	8
1988 Jul 27.3.....	47369.3	7.6625685(30)	*Ginga*	9
1989 Sep 13.5.....	47782.5	7.6610(2)	*Mir*/Kvant	10
1990 Apr 20.0	48001.0	7.660069(14)	*Ginga*	11
1990 Aug 30.5	48133.5	7.66001(4)	*ROSAT*	7
1990 Sep 25.5.....	48159.5	7.65989(45)	*Granat*/ART-P	12

REFERENCES.—(1) Joss et al. 1978; (2) Pravdo et al. 1979; (3) Li et al. 1980; (4) Elsner et al. 1983; (5) Nagase et al. 1984; (6) Kii et al. 1986; (7) Mavromatakis 1994; (8) Levine et al. 1988; (9) Shinoda et al. 1990; (10) Gilfanov et al. 1989; (11) Mihara 1995; (12) Lutovinov et al. 1994.

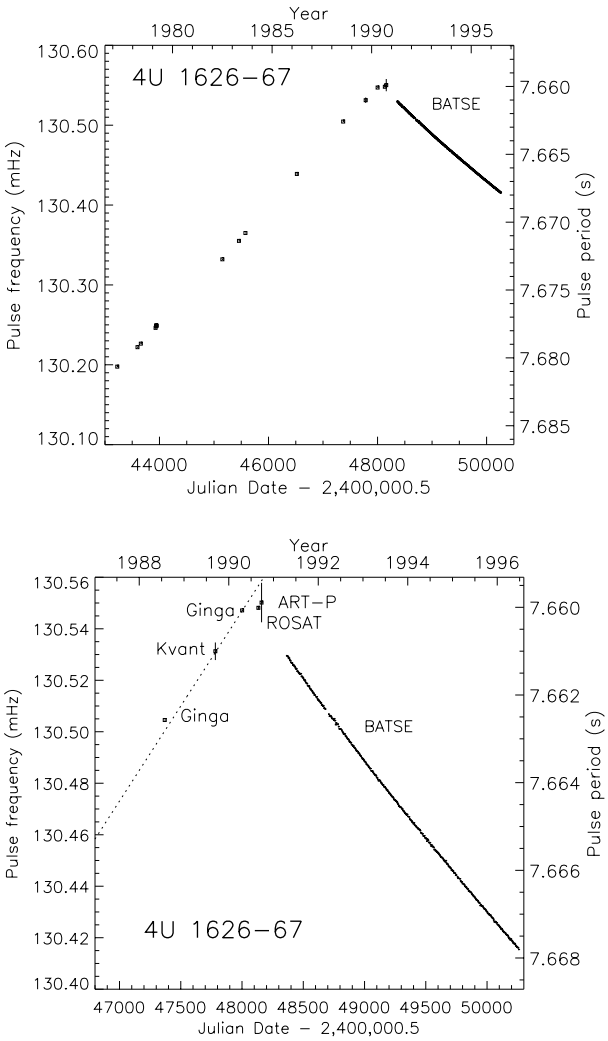

FIG. 1.—Pulse frequency history of 4U 1626−67, reduced to the solar system barycenter. Top panel shows the historical data, which are listed in Table 1. Bottom panel is an expanded view of the interval around the torque reversal and the BATSE observations. Dashed line shows the best linear fit to the 1977–1989 spin-up data (see text). Short gap in the BATSE history near MJD 48700 is due to the *Compton Gamma Ray Observatory* tape recorder failure.

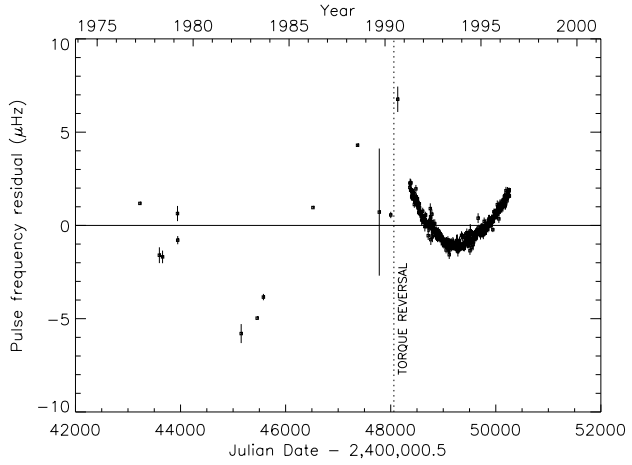

FIG. 2.—Long-term pulse frequency residuals with respect to a bimodal linear model with constant spin-up prior to MJD 48060 and constant spin-down after MJD 48060. Strong quadratic trend in the BATSE data is obvious, and a slower quadratic trend with the same curvature is apparent in the 1977–1986 data as well. The ∼4000 day timescale variation is probably due to ∼10% changes in the mass transfer rate.

the long-term spin-up and spin-down trends, we estimate that the torque reversal occurred during 1990 June. The 1990 observations by *Ginga* and *ROSAT* are especially constraining in this regard (see Figure 1, *bottom panel*).

The presence of a significant quadratic term in equation (1) indicates that the spin-down torque is decreasing in magnitude on the rapid timescale $|\dot{\nu}/\ddot{\nu}| \approx 26$ yr. Levine et al. (1988) reported that the spin-up torque was increasing on a similar timescale, $|\dot{\nu}/\ddot{\nu}| \approx 40$ yr, during 1977–1986. We note that the torque reversal from spin-up to spin-down occurred rapidly in comparison to these timescales. Despite the torque reversal between the two $\ddot{\nu}$ measurements, they both indicate the same sense of curvature in the torque history (i.e., $\ddot{\nu} > 0$ in both cases). In order to investigate the long-term behavior of $\ddot{\nu}$, we detrended the pulse frequency history with a bimodal linear model by assuming that the torque reversal occurred instantaneously at MJD 48060 and fitting the prereversal data with a constant spin-up trend, as well as the postreversal data, with a constant spin-down trend. The residuals with respect to this model are shown in Figure 2. (The 1979 February and 1990 September archival measurements are omitted because of their large measurement uncertainties and the presence of contemporaneous data of higher quality.) A quadratic trend in the BATSE observations is obvious, and a slower quadratic trend in the 1977–1986 data is apparent as well. Taken as a whole, the residuals appear to vary with ∼5 μHz amplitude on a 4000 day timescale.

The 4000 day variation in the frequency residuals cannot be due to orbital Doppler modulation, as we show here. The observed variation amplitude would imply a projected neutron star orbital radius of $a_X \sin i \approx 2100$ lt-s for $P_{orb} = 4000$ days, corresponding to a mass function of $f_X(M) \approx 0.8\ M_\odot$ for the companion. To fill its Roche lobe, such a companion would need to be an M supergiant, which is ruled out by the optical luminosity limits on the companion. The optical luminosity limits also rule out the possibility of a companion with a conventional wind (Chakrabarty 1996a). Therefore, we suggest that the 4000 day timescale in the frequency residuals reflects torque variations caused by ∼10% modulation of the mass transfer rate from the companion. Flux variations at this level are undetectable in the archival flux history of 4U 1626−67.

2.2. *Pulse Phases*

We can probe the rotation history of the pulsar more sensitively using a pulse arrival time (phase) analysis. We measured pulse phases by epoch-folding short (1–3 days) intervals of the DISCLA data and cross-correlating with a high signal-to-noise ratio pulse template. The pulsar's behavior is very stable, and we can maintain an unambiguous pulse count over the entire BATSE observation history. In the absence of a clear binary orbital signature, we fit the resulting pulse-phase history to a descriptive model of the form

$$\phi(t) = \phi_0 + \nu_0(t - t_0) + \tfrac{1}{2}\dot{\nu}_0(t - t_0)^2 + \tfrac{1}{6}\ddot{\nu}_0(t - t_0)^3 + \tfrac{1}{24}\dddot{\nu}(t - t_0)^4 , \quad (2)$$

where pulse phase is defined as the number of pulses since the epoch t_0, measured from the maximum of the funda-

mental harmonic of the 20–60 keV pulse profile. (The pulse shape is dominated by this harmonic.) The resulting best-fit parameters are as follows: $\phi_0 = 0.96138(2687)$, $\nu_0 = 0.130488503314(1211)$ Hz, $\dot{\nu}_0 = -7.1891352(3585) \times 10^{-13}$ Hz s^{-1}, $\ddot{\nu}_0 = 1.099875(3082) \times 10^{-21}$ Hz s^{-2}, and $\dddot{\nu} = 7.3424(1070) \times 10^{-30}$ Hz s^{-3}, referenced to the epoch $t_0 =$ MJD 49000 TDB. The pulse-phase residuals with respect to the fit to equation (2) are shown in Figure 3. Slowly varying excursions from the model on timescales of a few hundred days are evident. Quasi-periodic residuals with multiple zero crossings are a natural consequence of polynomial detrending of a red noise process (see below). We note that while the size and aperiodicity of the phase residuals limit the utility of equation (2) as a predictive pulse-phase ephemeris, equation (1) is an excellent (0.0002% rms residual) ephemeris for the pulse *frequency*.

The variation in the pulse-phase residuals is not periodic and therefore cannot arise from a binary orbit. Since the 42 minute orbit reported by Middleditch et al. (1981) has yet to be confirmed with pulse-timing measurements, it is interesting to use the Fourier amplitude spectrum of the pulse-phase residuals to set an upper limit on the possible size of a long-period orbit (see Levine et al. 1988). Because BATSE requires ~ 1 day to acquire a significant detection of 4U 1626−67, we cannot constrain the size of orbits with $P_{\rm orb} \lesssim 2$ days with our pulse-timing data. Combining our results with earlier measurements by *SAS 3*, *EXOSAT*, and *Ginga* (Rappaport et al. 1977; Joss, Avni, & Rappaport 1978; Levine et al. 1988; Shinoda et al. 1990), we can set the following upper limits on the projected orbital radius:

$$a_{\rm X} \sin i \lesssim \begin{cases} 8 \text{ lt-ms } (3\ \sigma) \\ \quad \text{for } P_{\rm orb} = 42 \text{ minutes } (\textit{Ginga}) \\ 13 \text{ lt-ms } (3\ \sigma) \\ \quad \text{for 10 minutes} \le P_{\rm orb} \le 10 \text{ hr } (\textit{EXOSAT}) \\ 100 \text{ lt-ms } (2\ \sigma) \\ \quad \text{for 1 day} \lesssim P_{\rm orb} \lesssim 2 \text{ days } (\textit{SAS 3}) \\ 60 \text{ lt-ms } (2\ \sigma) \\ \quad \text{for 2 days} \lesssim P_{\rm orb} \lesssim 60 \text{ days (BATSE)} \\ 150 \text{ lt-ms } (2\ \sigma) \\ \quad \text{for 60 days} \lesssim P_{\rm orb} \lesssim 900 \text{ days (BATSE)} . \end{cases} \quad (3)$$

The limit for orbital periods, $P_{\rm orb} \gtrsim 60$ days, is less stringent because of a substantial increase in noise power fluctuations at low frequencies. The polynomial detrending of the phase residuals (eq. [2]) limits our sensitivity to orbital motion on timescales comparable to our 1600 day observation length. For $P_{\rm orb} \gtrsim 900$ days, orbital modulations are adequately approximated by a fourth-order polynomial and thus cannot be separated from the long-term trends we observe in the spin frequency. For $P_{\rm orb} \lesssim 900$ days, the signature of a circular orbit cannot be represented by a fourth-order polynomial, and we find that the sensitivity is at most reduced by 30%. Losses due to trend removal are insignificant for $P_{\rm orb} \lesssim 500$ days. Our observations effectively rule out the possibility of a long-period orbit, lending strong support for the ultracompact binary model of 4U 1626−67.

2.3. *Noise Properties of the Pulse Phases*

Since the phase residuals in Figure 3 cannot be explained by a binary orbit, it is useful to characterize the statistical properties of the pulse-phase fluctuations. The strong correlations evident on long timescales indicate the presence of a strong "red noise" component (a power spectral component that rises with decreasing frequency) in the pulse-phase fluctuations. The presence of red noise can bias an unwindowed Fourier analysis of the power spectrum continuum because of power leakage through the broad sidelobe response of sinusoidal basis functions (Deeter & Boynton 1982). For a regularly sampled time series with no gaps, power spectral leakage can be suppressed (at a cost in frequency resolution) by judicious use of data windowing (Harris 1978). More sophisticated red noise spectral estimation techniques exist for handling data that are irregularly sampled or contain gaps (Deeter & Boynton 1982; Deeter 1984; Finger et al. 1996), but these are not required for the present analysis since our pulse-phase measurements for 4U 1626−67 are regularly sampled and continuous.

To achieve good suppression of the Fourier transform sidelobe response, we chose a multiplicative window function of the form

$$w_k = \cos^3 \left[\frac{(k - N/2)\pi}{N} \right], \quad (4)$$

with $k = 0, \ldots, N$. The windowed Fourier amplitudes are then given by

$$a_j = \frac{1}{N} \sum_{k=0}^{N-1} x_k w_k e^{-2\pi i j k/N} , \quad (5)$$

where x_k is the N-point equispaced time series of pulse-phase residuals in units of pulse cycles. The corresponding Fourier power is given by $|a_j|^2 (N/\sum w_k^2)$, where the factor in parentheses recovers the double-sided ($-f_{\rm Nyq} < f < f_{\rm Nyq}$) normalization of the power spectrum by enforcing Parseval's theorem with respect to the unwindowed time series. We obtain the power density spectrum (PDS) by dividing by the analysis frequency spacing, $\Delta f = (N \Delta t)^{-1}$. Polynomial detrending of a red noise process artificially suppresses power at very low frequencies. Numerical simulations showed that, for our case, only the lowest PDS bin is affected. We do not consider this bin in our analysis.

The resulting PDS of the pulse-phase fluctuations, P_ϕ, is shown in the left panel of Figure 4. A steep red noise spectrum dominates at low frequencies, while a white noise process caused by the statistical uncertainties in the pulse-phase measurements dominates above 10^{-7} Hz. Although our measurements were made of pulse phases, it is of physical interest to study the fluctuations in pulse frequency derivative, since this quantity is proportional to the net torque on the neutron star. The PDS of fluctuations in pulse frequency derivative $P_{\dot\nu}$ is simply related to P_ϕ by $P_{\dot\nu} = (2\pi f)^4 P_\phi$ (see, e.g., Boynton 1981). This spectrum, logarithmically rebinned in analysis frequency, is shown in the right panel of Figure 4. The error bars for the rebinned PDS data were determined using numerical simulations of similar red noise processes. The f^4 spectrum at analysis frequencies $f > 10^{-7}$ Hz is due to phase measurement noise. The spectrum turns over at lower frequencies, following a best-fit power law of $f^{-0.5 \pm 0.7}$.

Within the uncertainties, the low-frequency spectrum is consistent with white noise in the torque. This is equivalent to a random walk in pulse frequency of strength $S_\nu \equiv R\langle(\delta\nu)^2\rangle = P_{\dot\nu} = 10^{-21.5 \pm 0.3}$ Hz^2 s^{-1}, where R is the rate at which random walk steps of magnitude $\delta\nu$ occur. A fre-

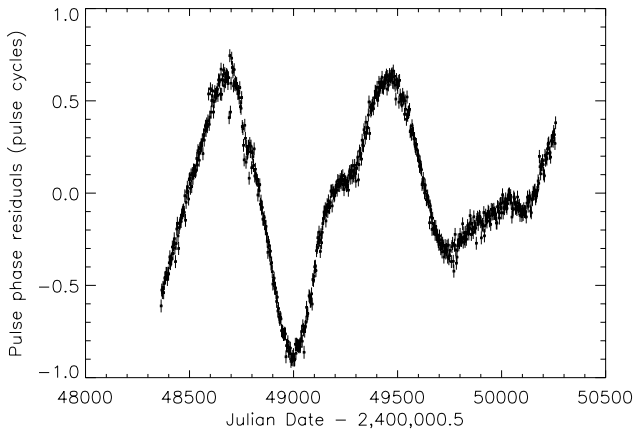

FIG. 3.—Pulse-phase residuals of 4U 1626−67 relative to the best-fit quartic phase model (eq. [2]). Phase measurements were obtained from 3 day folds of the 20–60 keV BATSE DISCLA data. Typical measurement uncertainty is ±0.035 pulse cycles. Large scatter in the measurements from the interval MJD 48600–48800 arises from reduced data quality associated with the *Compton Gamma Ray Observatory* tape recorder failure and subsequent telemetry gaps.

quency random walk is also observed in the accreting pulsars Her X-1 (Boynton 1981) and Vela X-1 (Deeter et al. 1989; Finger et al. 1996). If we write the individual random walk steps in frequency as $\Delta\nu_{\rm rw} = \dot{\nu}_{\rm rw}\,\tau_{\rm rw}$ (where $\tau_{\rm rw} = 1/R$ is the timescale on which the steps occur), then we find $|\dot{\nu}_{\rm rw}| = 0.047\,|\dot{\nu}_{\rm sd}|\,(\tau_{\rm rw}/1d)^{-1/2}$, where $\nu_{\rm sd}$ is the mean spin-down rate. Since we do not resolve any individual random walk steps in our pulse-phase observations, we cannot place any constraints on $\tau_{\rm rw}$.

We note, however, that our observations are also consistent with $1/f$ noise in the torque, as is also observed in the accreting pulsars Cen X-3 (Finger, Wilson, & Fishman 1994) and GX 1+4 (Chakrabarty et al. 1996). Because of the very low noise strength ($\sim 10^{-22}$ Hz^2 s^{-2} Hz^{-1}) in 4U 1626−67, only a small bandwidth interval of the BATSE data lies above the phase measurement noise level, leading to a large uncertainty in the power-law index for the torque noise.

Red noise processes are capable of inducing apparent high-order terms in the pulse-timing model. For example, the rms variation in the pulse frequency due to a random walk over a time T is $(S_\nu T)^{1/2}$. It is therefore of interest to know how large our observed values of $\dot{\nu}$, $\ddot{\nu}$, and $\dddot{\nu}$ are compared to the values expected as a result of red noise. We can set an approximate upper limit on the pulse frequency derivatives expected due to a frequency random walk by equating the rms frequency variation with the rms of the appropriate term in the Taylor expansion for frequency over our 1600 day observation. We find that the observed values of $\dot{\nu}$ and $\ddot{\nu}$ are too large to be induced by the inferred random walk strength, but the observed $\dddot{\nu}$ is consistent with being a red noise artifact.

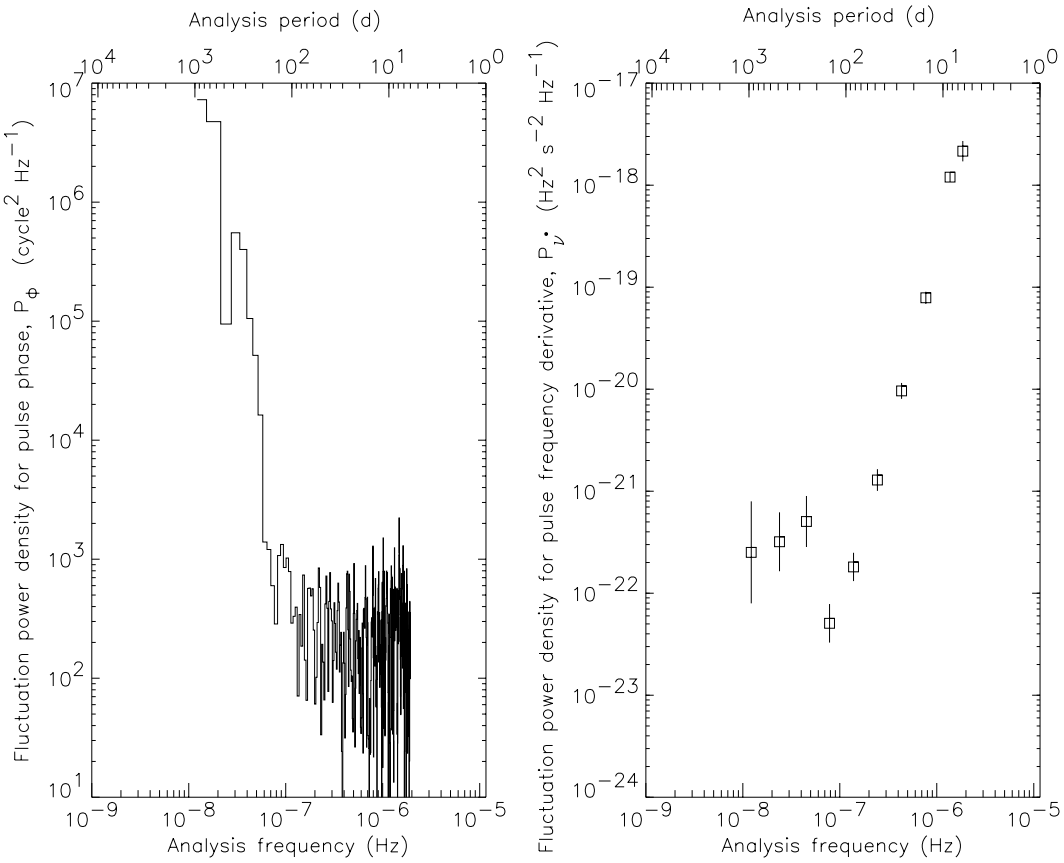

FIG. 4.—Fluctuation analysis of pulse-phase residuals of 4U 1626−67. *Left panel:* Power density spectrum of fluctuations in pulse phase 4U 1626−67. Steep red noise spectrum at low frequencies is torque noise intrinsic to the source, while the white noise spectrum above 10^{-7} Hz is due to pulse-phase measurement uncertainties. *Right panel:* Corresponding power density spectrum of fluctuations in the pulse frequency derivative $\dot{\nu}$, obtained by rescaling the spectrum on the left by $(2\pi f)^4$ and rebinning into uniform logarithmic intervals in frequency. The f^4 spectrum at high frequencies is due to the phase measurement noise. The relatively flat torque noise below 10^{-7} Hz has the smallest noise strength ever measured in an accreting pulsar.

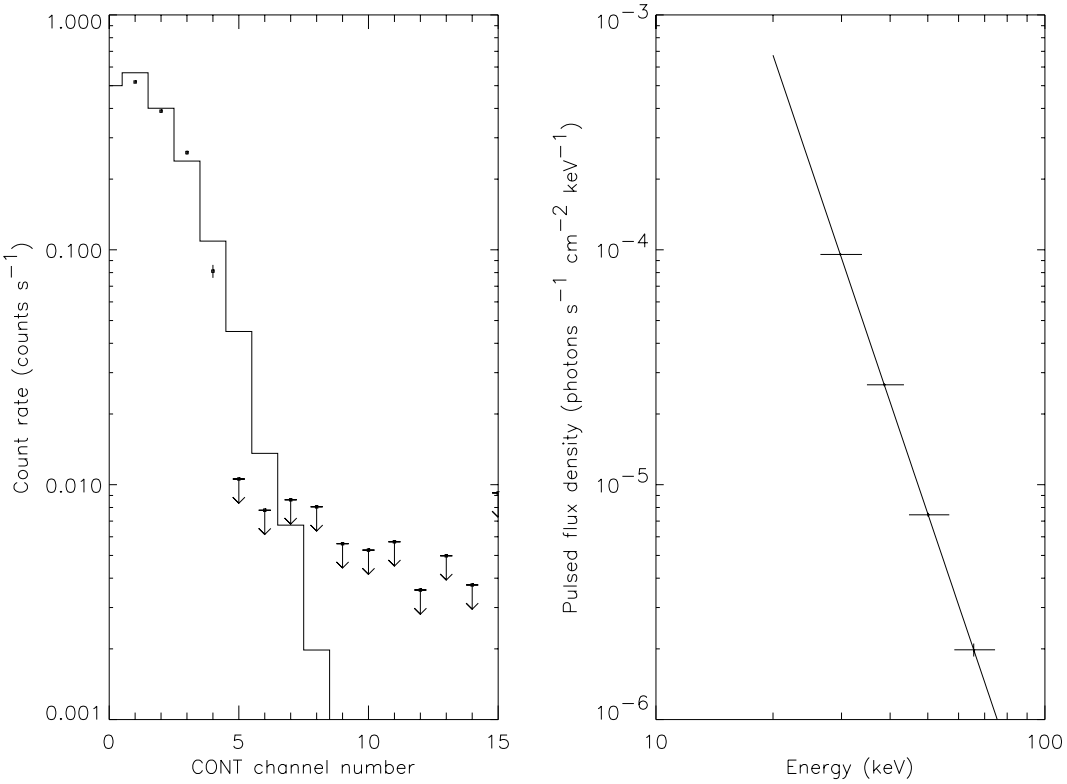

FIG. 5.—*Left panel:* Phase-averaged, pulsed count spectrum of 4U 1626−67 during the interval MJD 48370–49168. *Right panel:* Inferred phase-averaged, pulsed photon spectrum of 4U 1626−67 during the same interval. Vertical bars show the 1 σ statistical uncertainties, while the horizontal bars show the widths of the energy channels. Upper limits are quoted at 95% confidence. In both panels, the solid line shows the best-fit power-law photon spectral model ($\gamma = 4.91$, $C_{30} = 9.5 \times 10^{-5}$ photons cm^{-2} s^{-1} keV^{-1}).

2.4. *Spectral and Flux History of the Pulsed Emission*

In order to measure the photon energy spectrum of the pulsed emission, we folded a long segment of the BATSE CONT data (16 energy channels, 2.048 s resolution) using the pulse frequency model of equation (1). We used all the available data over the interval 1991 April 24 to 1993 June 30 (MJD 48370−49168). A single-harmonic pulse model was employed to measure the pulsed count rates in the pulse profiles (see Chakrabarty et al. 1995a). The inferred phase-averaged pulsed photon spectrum, assuming a power-law spectral model $dN/dE = C_{30}(E/30\,\mathrm{keV})^{-\gamma}$, is shown in Figure 5. The best-fit spectral parameters are $\gamma = 4.91(07)$ and $C_{30} = 9.5(1) \times 10^{-5}$ photons cm^{-2} s^{-1} keV^{-1}. This spectral index is consistent with the values measured in this energy range during spin-up, although the normalization constant is a factor of 4 smaller (Pravdo et al. 1979; Maurer et al. 1982). However, the archival observations were measuring both the pulsed and unpulsed components of the flux, so a direct comparison of their normalizations with ours is difficult. The pulse profiles from the CONT data (channels 1–5) are shown in Figure 6. No pulsed signal was detected in channel 5 or above. The detected pulsed count rate in channel 4 and the 95% confidence upper limits on the pulsed count rates for channels 5 and 6 all lie well below the extrapolation of the best-fit power-law model, suggesting the presence of a high-energy cutoff to the hard X-ray spectrum. (The steep $\gamma \approx 5$ power law observed above 20 keV in 4U 1626−67 itself represents a cutoff to the *soft* X-ray [1–20 keV] spectrum; see Pravdo et al. 1979.)

We obtained a 20–60 keV pulsed flux history by folding 5 day intervals of the DISCLA channel 1 data and correcting the resulting pulsed count rates for the BATSE instrumental response, assuming a fixed $\gamma = 4.9$ photon power-law spectrum. The resulting history, shown in Figure 7, was relatively steady at 1.5×10^{-10} ergs cm^{-2} s^{-1} over the entire BATSE observation interval, but with $\sim$50% variations over 50–100 day timescales. Unfortunately, we cannot use this history to make reliable inferences about the accretion rate onto the neutron star since the extremely steep hard X-ray spectrum results in a very large bolometric correction that is sensitive to small changes in the spectral index.

3. DISCUSSION

3.1. *Accretion Torques*

The accretion torque exerted on the neutron star in 4U 1626−67 is very steady, most likely a sign of disk accretion. Our observations have found that the neutron star is now steadily spinning down as it accretes, in contrast to the spin-up previously observed. This may indicate that the pulsar is spinning near its equilibrium period, where the magnetospheric radius is comparable to the corotation radius, $r_{co} = (GM_X/4\pi^2\nu^2)^{1/3} = 6.5 \times 10^8$ cm (assuming neutron star mass $M_X = 1.4\,M_\odot$). The characteristic torque $N_{char} = \dot{M} l_{co}$ is set by the mass accretion rate $\dot{M}$ and the specific angular momentum $l_{co} = (GM_X r_{co})^{1/2}$ of matter at the corotation radius. This torque would give a spin evolution rate of $|\dot{\nu}| = N/2\pi I \approx 3.5 \times 10^{-13}$ Hz s^{-1}, assuming $\dot{M} = 10^{-10}\,M_\odot$ yr^{-1} and moment of inertia $I = 10^{45}$ g cm^2. Since the actual torque might be less than N_{char}, we can use the value of $\dot{\nu}$ measured during spin-up to place a

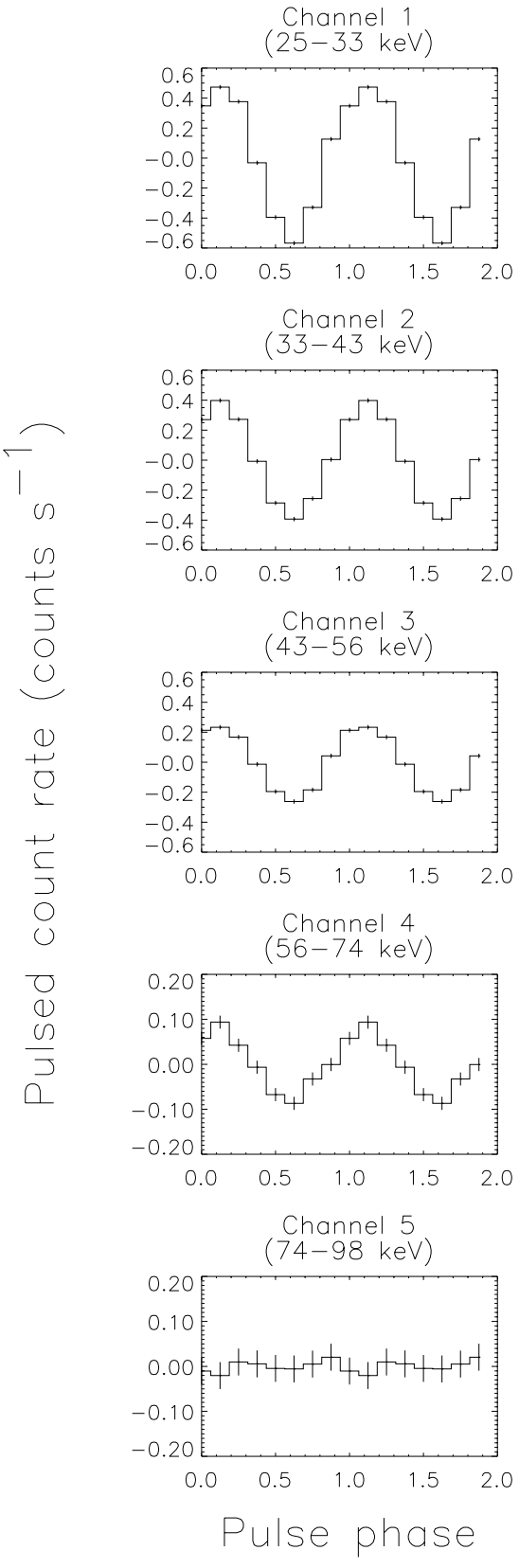

FIG. 6.—Pulse profiles as a function of energy for 4U 1626−67, averaged over the interval MJD 48370–49168. Two pulses are shown for each channel, and all channels are displayed relative to the same pulse phase. Mean energy edges for each CONT channel are indicated. These pulse profiles are overresolved by a factor of 2. Note that the pulse shapes are uncorrected for the rapid change in detector response as a function of energy in the 20–75 keV range. No pulse was detected in channel 5.

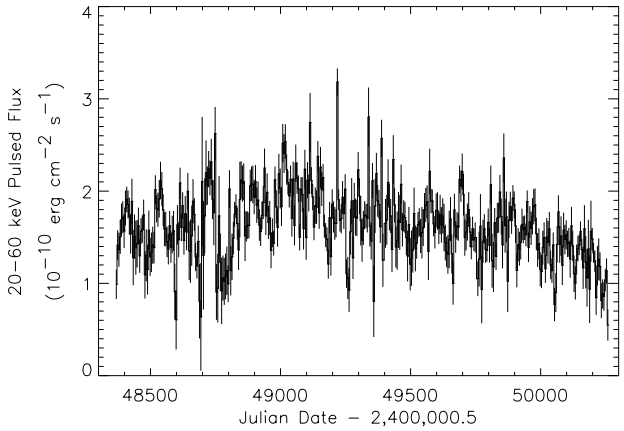

FIG. 7.—Pulse-phase–averaged 20–60 keV pulsed flux history of 4U 1626−67, assuming a $\gamma = 4.9$ photon power-law spectrum. Vertical bars show the 1 σ uncertainties in the flux measurements.

lower limit on the mass accretion rate, $\dot{M} \gtrsim 2 \times 10^{-10}\ M_\odot$ yr^{-1} (see Chakrabarty et al. 1993). As Levine et al. (1988) have already noted, mass accretion rates of this order are consistent with a low-mass degenerate helium or carbon-oxygen companion whose evolution is driven by gravitational radiation. To make this consistent with the best bolometric flux measurement during spin-up, $F_X \approx 2.4 \times 10^{-9}$ ergs cm^{-2} s^{-1} (0.7–60 keV; Pravdo et al. 1979), the source must be at least 3 kpc distant, lying more than 600 pc above the Galactic plane with a luminosity $\gtrsim 10^{36}$ ergs s^{-1}. The implied surface strength of the dipole magnetic field needed to place the magnetosphere at the corotation radius is $B \gtrsim 10^{12}$ G for these accretion rates. Although the magnetic field for this system has never been measured, previous authors have suggested a magnetic field strength of 6–8 $\times 10^{12}$ G on the basis of the cutoff energy in the X-ray spectrum (Pravdo et al. 1979) and the energy dependence of the pulse shape (Kii et al. 1986).

In the broader context of all the disk-fed accreting pulsars, a wide range of spin histories is seen (see Prince et al. 1994). Disk-fed pulsars with a characteristic spin-up time much shorter than their X-ray active lifetime should be at or near their equilibrium spin period. These systems evidently oscillate about this equilibrium through alternating episodes of spin-up and spin-down. We tested this hypothesis by comparing the observed long-term ($\gtrsim$years) mean torque $N_{\rm avg}$ to the characteristic torque $N_{\rm char}$. For 4U 1626−67, GX 1+4, SMC X-1, and 1E 2259+586 (all of which have exhibited steady long-term spin-up and/or spin-down behavior), we always find $N_{\rm avg} \gtrsim 0.2 N_{\rm char}$, which (within the uncertainties) is consistent with accretion from matter near the corotation radius. In contrast, for LMC X-4 (which also exhibits long-term spin-up over its sparsely sampled history), as well as Her X-1 and Cen X-3 (which have more erratic spin histories but with net spin-up), we find $N_{\rm avg} \sim 0.01 N_{\rm char}$. Some accreting pulsars have frequency histories that are consistent with a random walk (Baykal & Ögelman 1993), which could arise if the torque had a value $\sim N_{\rm char}$, but changed signs on a shorter timescale. Indeed, short timescale ($\lesssim$10–20 days) torque measurements for Her X-1 and Cen X-3 by BATSE always find torques well in excess of $N_{\rm avg}$, but never in excess of $N_{\rm char}$ (Wilson et al. 1994; Finger et al. 1994). This suggests that all disk-fed accreting pulsars show torques with magnitudes

$\lesssim N_{\rm char}$ on short timescales and differentiate themselves by the torque switching time.

3.2. *Torque Reversal*

It is unclear what physics sets the timescale for torque reversals. One possibility is the presence of long-term cycles in the supply of matter from the companion, which we have already suggested as the origin of the quasi-periodic fluctuations in pulse frequency shown in Figure 2. The various theories of magnetic accretion torques (Ghosh & Lamb 1979; Anzer & Börner 1983; Arons et al. 1984; Wang 1987; Lovelace, Romanova, & Bisnovatyi-Kogan 1995) all agree that lower values of the mass accretion rate will move the magnetosphere to larger radii and eventually lead to spin-down.

Long-term cycles in mass transfer are especially plausible if the ultracompact binary description of 4U 1626−67 is correct. The accretion rate is known to vary on 100–200 day timescales in the other two ultracompact X-ray sources, 4U 1820−30 and 4U 1916−05. The orbital period is much shorter in the 10 minute X-ray binary 4U 1820−30, where $\dot{M}$ varies by a factor of 3 [$\dot{M} \approx (2.5\text{–}7.5) \times 10^{-9}\ M_\odot\ \mathrm{yr}^{-1}$] on a 176 day cycle (Priedhorsky & Terrell 1984b). Priedhorsky & Terrell (1984a) also found a $\approx$50% modulation in the luminosity from the 50 minute X-ray binary 4U 1916−05 on a 199 day cycle. The origin of these superorbital modulations is still unknown. A comprehensive reanalysis of the *Vela 5B* database confirmed the 4U 1820−30 measurement, and marginally confirmed the 4U 1916−05 result (Smale & Lochner 1992). However, this reanalysis also showed that the luminosity from 4U 1626−67 did not vary by more than 15% on 100–200 day timescales. The BATSE 20–60 keV pulsed flux history does show $\sim$50% variations on 50–100 day timescales, but, as noted earlier, the large bolometric correction required for these data makes them an unreliable tracer of the mass accretion rate. Moreover, none of these observations address variations on timescales of order tens of years, which might be more relevant for 4U 1626−67.

We can examine archival observations of 4U 1626−67 to probe its long-term flux behavior. Table 2 summarizes all of the previous flux measurements. Only the 1978 *HEAO 1* observation was a broadband measurement, simultaneously covering 0.7–60 keV (Pravdo et al. 1979). The *HEAO 1* photon spectrum may be conveniently described by a broken power-law model with two break points, with photon indices $\gamma_1 \approx 1.6$ (0.7–10 keV), $\gamma_2 \approx 0.5$ (10–20 keV), and $\gamma_3 \approx 5$ (20–60 keV). For all of the 2–10 keV observations made prior to 1990, the spectral shape was consistent with the *HEAO 1* measurement. However, observations with both *Ginga* (Mihara 1995; Vaughan & Kitamoto 1996) and *ASCA* (Angelini et al. 1995) indicate that a dramatic change in the 2–10 keV spectral shape to a photon index $\gamma \lesssim 0.7$ occurred with the torque reversal in 1990. Although this implies a significant decrease in the 2–10 keV flux, the *Ginga*/ASM data also indicate that the shallow power law extends as far as 20 keV, so that it is not clear that the bolometric flux also decreased.

In order to make a comparison of the archival flux measurements, it is convenient to treat the *HEAO 1* observation as a fiducial and compare the other observations to the *HEAO 1* measurement in the appropriate bandpass. This ratio is given in the fifth column of Table 2 and plotted in Figure 8. For the *ASCA* measurement, we have extrapolated the observed 0.5–10 keV power law out to 20 keV, consistent with the 2–20 keV postreversal measurement of *Ginga*/ASM. The ratio data are consistent with constant intensity at the 2 σ level. However, there are indications of a gradual decline in intensity over the data span. In summary, while it is clear that the energy spectrum of 4U 1626−67 changed appreciably at the torque reversal, it is unclear whether the bolometric luminosity (and therefore the mass accretion rate) changed significantly as well. The anomalously high flux ratio value measured by *Ginga*/LAC (Mihara 1995) just prior to the torque reversal is intriguing.

The explanation that the torque reversal was caused by a change in the mass transfer rate from the companion is unsatisfactory in several other respects. For instance, it is curious that the torque magnitudes during spin-up and spin-down are so similar; the various theories of magnetic accretion torques predict that the torque would smoothly pass through zero before the magnetospheric radius moves

TABLE 2

4U 1626−67 Archival Flux History

Epoch			Bandpass			
Date	MJD	Instrument	(keV)	Flux[a]	Flux/*HEAO 1*[b]	Reference
Spin-up interval						
1977 Nov 24	43471	NRL balloon	18–50	8.3 ± 1.5	0.99 ± 0.21	1
1978 Mar 29	43596	*HEAO 1*/A-2	0.7–60	26 ± 3	1.00 ± 0.11	2
1979 Feb/Mar.....	43904–43963	*Einstein*/MPC	2–10	5.4 ± 0.3	0.72 ± 0.09	3
1983 May 4	45458	*Tenma*	2–20	10.7 ± 0.2	0.68 ± 0.08	4
1983 Aug 30.....	45576	*EXOSAT*	2–10	5.6 ± 0.5	0.75 ± 0.11	5
1987 Apr–1990 May.....	46885–48042	*Ginga*/ASM	2–20	8.9 ± 0.4	0.57 ± 0.10	6
1990 Apr 20	48001	*Ginga*/LAC	2–24	12.9 ± 0.1	0.80 ± 0.09	7
Spin-down interval						
1990 Jun–1991 Nov	48043–48591	*Ginga*/ASM	2–20	6.7 ± 0.6	0.42 ± 0.13	6
1993 Aug 11.....	49210	*ASCA*	0.5–10	2.9 ± 0.2	0.40 ± 0.08[c]	8

[a] In units of 10^{-10} ergs cm^{-2} s^{-1}.

[b] Ratio of measured flux and 1978 *HEAO 1* flux in the same bandpass.

[c] Flux ratio for 0.5–20 keV band, extrapolating the *ASCA* power-law fit to the 10–20 keV range. This is consistent with the 2–20 keV spectrum measured by *Ginga*/ASM (Vaughan & Kitamoto 1996).

References.—(1) Maurer et al. 1982; (2) Pravdo et al. 1979; (3) Elsner et al. 1983; (4) Kii et al. 1986; (5) Mavromatakis 1994; (6) Vaughan & Kitamoto 1996; (7) Mihara 1995; (8) Angelini et al. 1995.

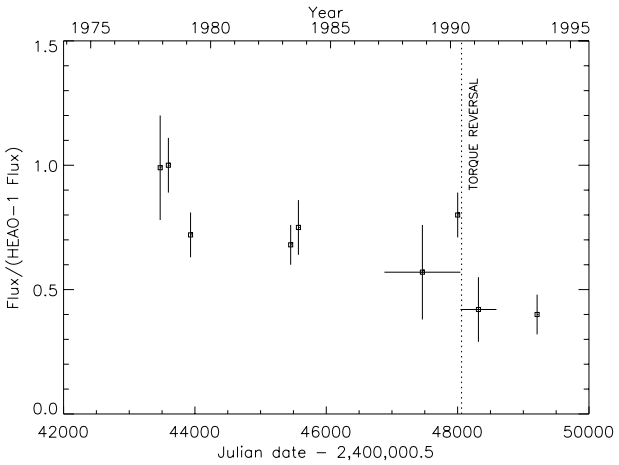

FIG. 8.—Long-term flux history of 4U 1626−67, relative to the flux measured by *HEAO 1* in the same bandpass. Individual measurements and bandpasses are listed in Table 2. Dotted line denotes the approximate epoch of the torque reversal.

outside the corotation radius (the point at which accretion might be halted by centrifugal effects), in which case one would expect a wide range of possible spin-down torque magnitudes. Moreover, one would expect the transition itself to be smooth and gradual, unless the change in the mass accretion rate were abrupt. As such, it is difficult to reconcile the abrupt change in torque from spin-up to spin-down with the extremely smooth spin-down torque that BATSE has observed for several years. A similarly abrupt change in the rate of mass loss from the companion seems unlikely in an ultracompact binary, since the mass transfer is driven by gravitational radiation. An adequate explanation may require a new model, where both the torque reversal and any accretion rate change are explained by a change of state in the neutron star accretion disk system rather than a change in the companion. Possibilities include disk-magnetosphere instabilities or changes in the field configuration of the neutron star.

3.3. *Internal Torques and Timing Noise*

The neutron star in accreting X-ray pulsars is subject to both external and internal torques. The external torques arise from both the accretion of matter from the binary companion and the interaction of the pulsar magnetosphere with the accretion disk. The internal torques arise from the response of the neutron star to these external torques and depend on the detailed interior structure of neutron stars. The pulse phase and its time derivatives provide a probe of these torque components. Among the accretion-powered pulsars, detailed statistical studies have been made of the disk-fed systems Her X-1 (Boynton 1981), Cen X-3 (Finger et al. 1994), and GX 1+4 (Chakrabarty et al. 1996), as well as the wind-fed system Vela X-1 (Deeter et al. 1989; Finger et al. 1996). Her X-1 and Vela X-1 both exhibit fluctuations consistent with a random walk in pulse frequency of strength 2×10^{-19} Hz^2 s^{-1} and 2×10^{-20} Hz^2 s^{-1}, respectively. The PDS of torque fluctuations for both Cen X-3 and GX 1+4 exhibit $1/f$ noise with strength greater than 10^{-18} Hz^2 s^{-2} Hz^{-1} below 10^{-6} Hz. It is unclear from our observations which type of torque noise process is operative in 4U 1626−67, but, in either case, the $\sim 10^{-22}$ Hz^2 s^{-2} Hz^{-1} strength at 10^{-7} Hz indicates that the process is very quiet; in fact, this is the smallest noise strength ever measured in an accretion-powered pulsar. These contrasts may simply reflect differences in the stability of the accretion flows in these systems.

The torque noise seen in 4U 1626−67 is comparable to the timing irregularities seen in many young radio pulsars (see Lyne 1993 for a review). The timing noise in most of these radio pulsars can also be described by a random walk in frequency (Cordes & Helfand 1980), with the Crab pulsar (one of the youngest and noisiest) exhibiting a 7×10^{-23} Hz^2 s^{-1} random walk in frequency (Boynton et al. 1972; Cordes & Helfand 1980), less than a factor of 10 weaker than what we observe in 4U 1626−67. Observations of glitches and timing noise in radio pulsars have motivated much theoretical work on the interactions between the crustal neutron superfluid and the charged component of the crust (see Alpar 1995 for a recent summary). Current models depend on the strength of the torque and (via activation energies) the core temperature of the neutron star (see Alpar & Pines 1988). Whether the torque is caused by accretion or by a rotating magnetic dipole is most likely irrelevant, raising the interesting possibility of observing similar effects in accreting systems (Lamb, Pines, & Shaham 1978). Internal torques might be the source of the noise process we observe in 4U 1626−67.

The noisiest radio pulsars are young ($\lesssim 10^4$ yr; Lyne 1993) and still have relatively hot cores from birth ($T_c \gtrsim 2 \times 10^8$ K for a standard cooling curve; see Nomoto & Tsuruta 1987). The core temperature in an accreting neutron star is also $\gtrsim 10^8$ K, as the nuclear burning of the freshly accreted matter on the surface heats the interior to these temperatures in less than 10^6 yr (Fujimoto et al. 1984). For the global accretion rate of $10^{-10}\ M_\odot$ yr^{-1} rate relevant to 4U 1626−67, the steady state core temperature should be $T_c \approx 1 \times 10^8$ K (Ayasli & Joss 1982). On the other hand, the external torques in young radio pulsars are generally larger than what we observe in 4U 1626−67 ($\dot{\nu} = 3.6 \times 10^{-10}$ Hz s^{-1} in the Crab pulsar). Even though the torques are different, it remains to be seen whether the hot core of an accreting neutron star can produce timing noise like that seen in young radio pulsars. In order to test this idea with 4U 1626−67, a careful correlation of the torque with the bolometric luminosity will be necessary so that variability in the accretion rate can be eliminated as a possible source of the torque noise.

4. SUMMARY

We have shown that 4U 1626−67 underwent an abrupt torque reversal in 1990, switching to steady spin-down after 13 yr of steady spin-up. The current spin-down rate is nearly equal to the previous spin-up rate, with a spin evolution timescale of $|\nu/\dot{\nu}| \approx 5000$ yr in both states. The long-term spin history also contains small amplitude fluctuations on a 4000 day timescale, which are probably caused by variations in the mass transfer rate from the companion. On shorter timescales, the torque history of 4U 1626−67 is exceptionally smooth, comparable in strength to the timing noise measured in young radio pulsars.

It is unclear what caused the torque reversal. There is no clear evidence for a change in the mass transfer rate, although the X-ray spectrum changed significantly. The abruptness of the reversal and the similarity of the spin-up and spin-down magnitudes are difficult to explain in terms of a gradual change in $\dot{M}$, while an abrupt change in $\dot{M}$ is hard to imagine in an ultracompact binary, where mass

transfer is driven by gravitational radiation. Pulse-timing analysis of the BATSE observations effectively rule out long binary periods, lending support for the ultracompact binary model of 4U 1626−67.

It is a pleasure to thank Rob Nelson for useful discussions. We also thank the referee, Michiel van der Klis, for a careful reading of the manuscript. This work was funded in part by NASA grants NAG 5-1458 and NAGW-4517. D. C. was supported by a NASA GSRP Graduate Fellowship under grant NGT-51184 and by a NASA Compton Postdoctoral Fellowship under grant NAG 5-3109. L. B. was supported by Caltech's Lee A. DuBridge Fellowship, funded by the Weingart Foundation; by a NASA Compton Postdoctoral Fellowship under grant NAG 5-2666; and by the Alfred P. Sloan Foundation.

APPENDIX A

DECOHERENCE TIMESCALES IN PULSE TIMING

It is often necessary to integrate weak signals over long observations in order to obtain a significant detection. For pulse-timing observations of a source whose pulse frequency[6] is not constant, this can lead to signal decoherence as later pulses are integrated out of phase with earlier pulses; it does not matter whether the measurement is in the time domain (epoch folding) or in the frequency domain (power spectra). Decoherence effects degrade sensitivity and can lead to nondetection for sufficiently weak signals. In this appendix, we calculate the timescale on which a signal decoherence becomes important. Observation lengths comparable to this timescale will suffer loss of sensitivity as a result of pulse smearing, unless steps are taken to maintain pulse-phase coherence. This effect can render threshold signals undetectable unless steps are taken to preserve phase coherence. Pulse shapes with short duty cycles are considerably more susceptible to this problem. For accretion-powered pulsars, there are two common causes of signal decoherence: accretion torques and orbital Doppler shifts.

Let us first consider the effect of a constant frequency derivative $\dot{\nu}$ on a pulse-timing observation. The pulse phase (in cycles) is given by

$$\phi = \phi_0 + \dot{\phi}t + \tfrac{1}{2}\ddot{\phi}t^2 + \cdots \tag{A1}$$

$$= \phi_0 + \nu t + \tfrac{1}{2}\dot{\nu}t^2 + \cdots , \tag{A2}$$

where we define decoherence as having reached a phase residual $\Delta\phi = \frac{1}{2}$ with respect to the optimal constant frequency model. Then the decoherence condition can be written

$$\Delta\phi = \tfrac{1}{2}\dot{\nu}\tau^2 = \tfrac{1}{2} , \tag{A3}$$

and the decoherence timescale is

$$\tau_{\rm decoh} = \sqrt{\frac{1}{\dot{\nu}}} = \sqrt{\frac{P^2}{\dot{P}}} . \tag{A4}$$

In the case of 4U 1626−67, $\tau_{\rm decoh} \approx 13$ days. For longer observations, phase coherence can be recovered by "accelerating" the time series to compensate for the phase drift, essentially stretching or squeezing the size of the time bins (Middleditch 1989; Anderson et al. 1990; Wood et al. 1991; Johnston & Kulkarni 1991; Vaughan et al. 1994).

A second cause of signal decoherence is periodic Doppler shifting of the pulse frequency due to a binary orbit. We restrict our discussion to the case of a circular orbit, where the pulse phase can be written

$$\phi = \phi_0 + \dot{\phi}t + \frac{(a_{\rm X}/c)\,\sin i}{P_{\rm pulse}} \cos\left(\frac{2\pi t}{P_{\rm orb}} + \psi\right) \tag{A5}$$

$$= \phi_0 + \nu t + \frac{(a_{\rm X}/c)\,\sin i}{P_{\rm pulse}} \left[1 - \frac{1}{2}\left(\frac{2\pi t}{P_{\rm orb}} + \psi\right)^2 + \frac{1}{4!}\left(\frac{2\pi t}{P_{\rm orb}} + \psi\right)^4 + \cdots\right], \tag{A6}$$

and the corresponding decoherence condition is given by

$$\Delta\phi = \frac{(a_{\rm X}/c)\,\sin i}{P_{\rm pulse}} \left[1 - \cos\left(\frac{2\pi\tau}{P_{\rm orb}} + \psi\right)\right] = \frac{1}{2} . \tag{A7}$$

Since we are interested in the *minimum* decoherence timescale, we set the orbital phase $\psi = 0$. Then the orbital decoherence timescale is

$$\tau_{\rm decoh} = P_{\rm orb}\,\frac{1}{2\pi}\cos^{-1}\left[1 - \frac{1}{2}\,\frac{P_{\rm pulse}}{(a_{\rm X}/c)\,\sin i}\right] \quad \text{(exact)} . \tag{A8}$$

[6] The relevant quantity is *pulse* frequency rather than spin frequency. In the BATSE 20–60 keV energy band, this distinction is important since some pulsars (e.g., Vela X-1) are predominantly seen at $\nu_{\rm pulse} = 2\nu_{\rm spin}$.

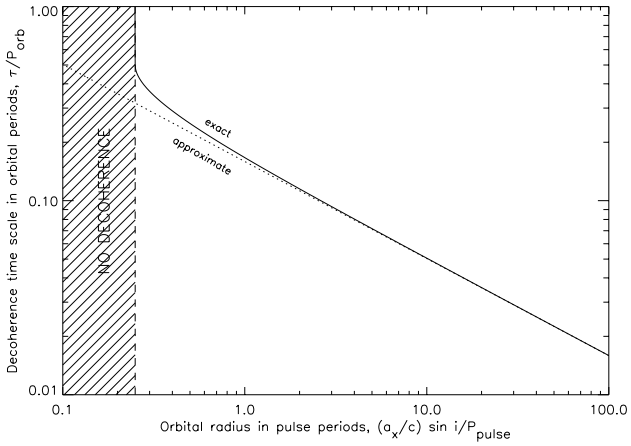

FIG. 9.—Decoherence timescale due to orbital motion as a function of projected orbital radius. Solid curve shows the exact solution from eq. (A8), and the dotted curve shows the approximate solution from eq. (A9). Shaded region indicates the location of systems that are not subject to orbital decoherence. Assuming that the projected radius of 4U 1626−67 is bounded by (a_X/c) sin $i/P_{pulse} < 0.001$, it must lie in this region.

TABLE 3

ORBITAL DECOHERENCE TIMESCALES

System	P_{pulse} (s)	P_{orb} (days)	a_X sin i (lt-s)	$[(a_X/c)$ sin $i]/P_{pulse}$	τ_{decoh} (hr)
GRO J1744−28	0.467	11.8	2.63	5.6	19.1
SMC X-1	0.7	3.89	53.5	76.4	1.70
Her X-1	1.2	1.7	13.2	11	1.96
Cen X-3	4.8	2.09	39.6	8.2	2.79
4U 1626−67	7.7	0.02	<0.008	<0.001	∞
GS 0834−430	12.3	111	205.7	16.7	103.9
LMC X-4	13.5	1.408	26.3	1.9	3.94
OAO 1657−415	37.7	10.4	106	2.8	24.1
Vela X-1	141[a]	8.96	113.6	0.8	40.4
4U 1907+09	438	8.38	80.2	0.18	∞
4U 1538−52	530	3.73	52.8	0.1	∞

[a] Second harmonic (dominant at BATSE energies).

This expression can be simplified for two special cases. If the light travel time across the orbit is long compared to the pulse period, then

$$\tau_{decoh} \approx \frac{P_{orb}}{2\pi}\left[\frac{P_{pulse}}{(a_X/c)\sin i}\right]^{1/2} \quad \text{for} \quad \frac{(a_X/c)\sin i}{P_{pulse}} \gtrsim \frac{1}{2}. \tag{A9}$$

However, for sufficiently small orbits $[(a_X/c)\sin i < P_{pulse}/4]$, the signal will not suffer from decoherence at all ($\tau_{decoh} = \infty$). Note that these calculations are not accurate for highly eccentric orbits.

The critical quantity that determines the importance of decoherence effects is clearly the ratio $(a_X/c)\sin i/P_{pulse}$. A plot of orbital decoherence timescale in orbital periods, as a function of this ratio, is shown in Figure 9. For 4U 1626−67, the upper limit on the projected light travel time across the orbit is so small compared to the pulse period that the pulsar signal will never lose coherence due to binary motion. The decoherence timescales for a number of other low-eccentricity accreting pulsar systems is given in Table 3.

REFERENCES

Alpar, M. A. 1995, in The Lives of Neutron Stars, ed. M. A. Alpar et al. (Dordrecht: Kluwer), 185
Alpar, M. A., & Pines, D. 1988, in Timing Neutron Stars, ed. H. Ogelman & E. P. J. van den Heuvel (Dordrecht: Kluwer), 441
Anderson, S. B., et al. 1990, Nature, 346, 42
Angelini, L., Ghosh, P., & White, N. E. 1994, in New Horizon of X-Ray Astronomy, ed. F. Makino & T. Ohashi (Tokyo: Univ. Acad. Press), 411
Angelini, L., White, N. E., Nagase, F., Kallman, T. R., Yoshida, A., Takeshima, T., Becker, C. M., & Paerels, F. 1995, ApJ, 449, L41
Anzer, U., & Börner, G. 1983, A&A, 122, 73
Arons, J., Burnard, D., Klein, R. I., McKee, C. F., Pudritz, R. E., & Lea, S. M. 1984, in High Energy Transients in Astrophysics, ed. S. E. Woosley (New York: AIP), 215
Ayasli, S., & Joss, P. C. 1982, ApJ, 256, 637
Baykal, A., & Ögelman, H. 1993, A&A, 267, 119
Bildsten, L., Chakrabarty, D., Chiu, J., Finger, M. H., Grunsfeld, J. M., Koh, T., Prince, T. A., & Wilson, R. B. 1994, in Second Compton Symp., ed. C. E. Fichtel, N. Gehrels, & J. P. Norris (New York: AIP), 290
Boynton, P. E. 1981, in Pulsars, ed. W. Sieber & R. Wielebinski (Dordrecht: Reidel), 279
Boynton, P. E., Groth, E. J., Hutchinson, D. P., Nanos, G. P., Partridge, R. B., & Wilkinson, D. T. 1972, ApJ, 175, 217
Bradt, H. V., Apparao, K. M. V., Dower, R., Doxsey, R. E., Jernigan, J. G., & Markert, T. H. 1977, Nature, 269, 496
Chakrabarty, D. 1996a, in preparation
———. 1996b, Ph.D. thesis, California Institute of Technology
Chakrabarty, D., et al. 1993, ApJ, 403, L33
———. 1996, ApJ, in preparation
Chakrabarty, D., Koh, T., Bildsten, L., Prince, T. A., Finger, M. H., Wilson, R. B., Pendleton, G. N., & Rubin, B. C. 1995a, ApJ, 446, 826

Chakrabarty, D., Koh, T., Prince, T. A., Vaughan, B., Finger, M. H., Scott, M., & Wilson, R. B. 1995b, IAU Circ. 6153
Chakrabarty, D., Prince, T. A., Finger, M. H., & Wilson, R. B. 1994, IAU Circ. No. 6105
Chester, T. J. 1979, ApJ, 227, 569
Cordes, J. M., & Helfand, D. J. 1980, ApJ, 239, 640
Deeter, J. E. 1984, ApJ, 281, 482
Deeter, J. E., & Boynton, P. E. 1982, ApJ, 261, 337
Deeter, J. E., Boynton, P. E., Lamb, F. K., & Zylstra, G. 1989, ApJ, 336, 376
Elsner, R. F., Darbro, W., Leahy, D., Weisskopf, M. C., Sutherland, P. G., Kahn, S. M., & Grindlay, J. E. 1983, ApJ, 266, 769
Elsner, R. F., Ghosh, P., & Lamb, F. K. 1980, ApJ, 241, L155
Finger, M. H., Vaughan, B., van der Klis, M., Berger, M., & Wilson, R. B. 1996, ApJ, submitted
Finger, M. H., Wilson, R. B., & Fishman, G. J. 1994, in Second Compton Symp., ed. C. E. Fichtel, N. Gehrels, & J. P. Norris (New York: AIP), 304
Fishman, G. J., et al. 1989, in Proc. Gamma Ray Obs. Sci. Workshop, ed. W. N. Johnson (Greenbelt: NASA/GSFC), 2-39
Fujimoto, M. Y., Hanawa, T., Iben, I., & Richardson, M. B. 1984, ApJ, 278, 813
Ghosh, P., & Lamb, F. K. 1979, ApJ, 234, 296
Giacconi, R., Murray, S., Gursky, H., Kellogg, E., Schreier, E., & Tananbaum, H. 1972, ApJ, 178, 281
Gilfanov, M., et al. 1989, in Proc. 23rd ESLAB Symp. on Two Topics in X-Ray Astronomy, Vol. 1 (Noordwijk: ESA SP–196), 71
Harris, F. J. 1978, Proc. IEEE, 66, 51
Ilovaisky, S. A., Motch, C., & Chevalier, C. 1978, A&A, 70, L19
Johnston, H. M., & Kulkarni, S. R. 1991, ApJ, 368, 504
Joss, P. C., Avni, Y., & Rappaport, S. 1978, ApJ, 221, 645
Kii, T., Hayakawa, S., Nagase, F., Ikegami, T., & Kawai, N. 1986, PASJ, 38, 751
Lamb, F. K., Pines, D., & Shaham, J. 1978, ApJ, 224, 969
Levine, A., Ma, C. P., McClintock, J., Rappaport, S., van der Klis, M., & Verbunt, F. 1988, ApJ, 327, 732
Li, F. K., Joss, P. C., McClintock, J. E., Rappaport, S., & Wright, E. L. 1980, ApJ, 240, 628
Lovelace, R. V. E., Romanova, M. M., & Bisnovatyi-Kogan, G. S. 1995, MNRAS, 275, 244
Lutovinov, A. A., Grebenev, S. A., Sunyaev, R. A., & Pavlinsky, M. N. 1994, Astron. Lett., 20, 538
Lyne, A. G. 1993, in Pulsars as Physics Laboratories, ed. R. D. Blandford et al. (Oxford: Oxford Univ. Press), 29
Makishima, K., et al. 1988, Nature, 333, 746
Maurer, G. S., Johnson, W. N., Kurfess, J. D., & Strickman, M. S. 1982, ApJ, 254, 271
Mavromatakis, F. 1994, A&A, 285, 503
McClintock, J. E., Canizares, C. R., Bradt, H. V., Doxsey, R. E., Jernigan, J. G., & Hiltner, W. A. 1977, Nature, 270, 320
McClintock, J. E., Canizares, C. R., Li, F. K., & Grindlay, J. E. 1980, ApJ, 235, L81
Middleditch, J. 1989, in Supercomputing '89, Vol. 2, ed. L. P. Kartashev & S. I. Kartashev (St. Petersburg, FL: Intl. Supercomp. Inst.), 303
Middleditch, J., Mason, K. O., Nelson, J. E., & White, N. E. 1981, ApJ, 244, 1001
Mihara, T. 1995, Ph.D. thesis, Univ. Tokyo
Nagase, F., et al. 1984, PASJ, 36, 667
Nelson, L. A., Rappaport, S. A., & Joss, P. C. 1986, ApJ, 304, 231
Nomoto, K., & Tsuruta, S. 1987, ApJ, 312, 711
Pravdo, S. H., et al. 1979, ApJ, 231, 912
Priedhorsky, W. C., & Terrell J. 1984a, ApJ, 280, 661
———. 1984b, ApJ, 284, L17
Prince, T. A., Bildsten, L., Chakrabarty, D., Wilson, R. B., & Finger, M. H. 1994, in Evolution of X-Ray Binaries, ed. S. S. Holt & C. S. Day (New York: AIP), 235
Rappaport, S., Markert, T., Li, F. K., Clark, G. W., Jernigan, J. G., & McClintock, J. E. 1977, ApJ, 217, L29
Shinoda, K., Kii, T., Mitsuda, K., Nagase, F., Tanaka, Y., Makishima, K., & Shibazaki, N. 1990, PASJ, 42, L27
Smale, A. P., & Lochner, J. C. 1992, ApJ, 395, 582
Standish, E. M., Newhall, X. X., Williams, J. G., & Yeomans, D. K. 1992, in Explanatory Supplement to the Astronomical Almanac, ed. P. K. Seidelmann (Mill Valley: University Science), 279
Vaughan, B. A., et al. 1994, ApJ, 435, 362
Vaughan, B. A., & Kitamoto, S. 1996, in preparation
Verbunt, F., Wijers, R. A. M. J., & Burm, H. M. G. 1990, A&A, 234, 195
Wang, Y. M. 1987, A&A, 183, 257
Warner, B. 1995a, Ap&SS, 225, 249
———. 1995b, Cataclysmic Variable Stars (Cambridge: Cambridge Univ. Press)
Wilson, R. B., Finger, M. H., Pendleton, G. N., Briggs, M., & Bildsten, L. 1994, in Second Compton Symp., ed. C. E. Fichtel, N. Gehrels, & J. P. Norris (New York: AIP), 235
Wilson, R. B., Fishman, G. J., Finger, M. H., Pendleton, G. N., Prince, T. A., & Chakrabarty, D. 1993, in *Compton Gamma Ray Observatory*, ed. M. Friedlander, N. Gehrels, & D. J. Macomb (New York: AIP), 291
Wood, K. S., et al. 1991, ApJ, 379, 295